European Journal of Applied Physiology
https://doi.org/10.1007/s00421-019-04251-1

ORIGINAL ARTICLE

Neuromechanical adjustments when walking with an aiding or hindering horizontal force

A. H. Dewolf[1,2] · Y. P. Ivanenko[3] · R. M. Mesquita[1] · F. Lacquaniti[2,3] · P. A. Willems[1]

Received: 30 July 2019 / Accepted: 28 October 2019

Abstract

Purpose Walking against a constant horizontal traction force which either hinders or aids the motion of the centre of mass of the body (COM) will create a discrepancy between the positive and negative work being done by the muscles and may thus affect the mechanics and energetics of walking. We aimed at investigating how this imbalance affects the exchange between potential and kinetic energy of the COM and how its dynamics is related to specific spatiotemporal organisation of motor pool activity in the spinal cord. To understand if and how the spinal cord activation may be associated with COM dynamics, we also compared the neuromechanical adjustments brought on by a horizontal force with published data about those brought on by a slope.

Methods Ten subjects walked on a treadmill at different speeds with different traction forces. We recorded kinetics, kinematics, and electromyographic activity of 16 lower-limb muscles and assessed the spinal locomotor output by mapping them onto the rostrocaudal location of the motoneuron pools.

Results When walking with a hindering force, the major part of the exchange between potential and kinetic energy of the COM occurs during the first part of stance, whereas with an aiding force exchanges increase during the second part of stance. Those changes occur since limb and trunk orientations remain aligned with the average orientation of the ground reaction force vector. Our results also show the sacral motor pools decreased their activity with an aiding force and increased with a hindering one, whereas the lumbar motor pools increased their engagement both with an aiding and a hindering force.

Conclusion Our findings suggest that applying a constant horizontal force results in similar modifications of COM dynamics and spinal motor output to those observed when walking on slopes, consistent with common principles of motor pool functioning and biomechanics of locomotion.

Keywords Neuromechanics · Braking and propulsion force · Spinal maps · Pendular energy exchange · COM dynamics

Communicated by Jean-René Lacour.

✉ P. A. Willems
patrick.willems@uclouvain.be

[1] Laboratory of Biomechanics and Physiology of Locomotion, Institute of Neuroscience, Université Catholique de Louvain (UCL-FSM), Place P. de Coubertin, 1, 1348 Louvain-la-Neuve, Belgium

[2] Department of Systems Medicine and Center of Space Biomedicine, University of Rome Tor Vergata, 00133 Rome, Italy

[3] Laboratory of Neuromotor Physiology, IRCCS Santa Lucia Foundation, 00179 Rome, Italy

Abbreviations

β_F	Orientation of the average GRF relative to the vertical
a_l, a_v, a_f	Lateral, vertical and fore–aft acceleration of the COM
BW	Body weight
COM	Centre of mass of the whole body, the point where the weighted relative position of a distributed mass sums to zero
E_{kf}, E_{kv}, E_{kl}	Energy due to the fore–aft, vertical and lateral movement of the COM
EMG	Records of the electrical activity produced by skeletal muscles
E_p^*	Potential energy of the COM
E_s	'Pendular energy savings', amount of energy saved by the pendular energy exchange

Published online: 07 November 2019

$\dot{e}(t)$	Rate of pendular energy savings, which represents the magnitude of energy exchanged
FC	Foot contact
F_f, F_l, F_v	Fore–aft, lateral and vertical component of the GRF
F_t	Horizontal traction force
GRF	Ground reaction force
L	Stride length
m	Body mass
$r(t)$	Recovery within the step, which evaluates the E_p–E_k transduction (in %) at each instant of the walking step
h	Vertical displacement of the COM
TO	Toe off
v_{belt}	Velocity of the belt
v_l, v_v, v_f	Lateral, vertical and fore–aft velocity of the COM
$\dot{W}_1^+$ and $\dot{W}_2^+$	First and second peak of positive power during a step, respectively
$\dot{W}^-$	Major peak of negative power during a step
W_{ext}	Work done by the subject to move the COM relative to the surroundings
$\dot{W}_{ext}$	Power used by the subject to move the COM relative to the surroundings
W_t	Work done by the horizontal traction force

Introduction

The metabolic cost of walking depends on, amongst others, mechanical tasks such as supporting body weight, producing force to decelerate (braking) and accelerate (propulsion) the centre of mass of the body (COM) forwards and swinging the limbs. When walking on level, firm ground and at a constant speed, muscles perform as much positive as negative work to move the body relative to the environment (Cavagna et al. 1976). However, in nature, this situation is rather infrequent [e.g., moving against the wind (Pugh 1971), on sand (Lejeune et al. 1998), or on slopes (Dewolf et al. 2016)]. Several studies have then been carried out providing a detailed analysis of the effect of changing the balance between positive and negative work. For example, changing the speed of progression (e.g., Ivanenko et al. 2006, 2013a; Van Caekenberghe et al. 2013) or the slope of the terrain (e.g., Sun et al. 1996; Franz and Kram 2013) are common natural perturbations to propulsion and braking demands.

During walking, the speed and slope affect the pendular energy exchange of the COM and thus the mechanical power developed throughout the step (Gottschall and Kram 2006; Dewolf et al. 2017). In 2010, Cappellini et al. showed that the pendular dynamics correlated with the spatiotemporal progression of motor pool activity rostrocaudally in the spinal cord. Therefore, Dewolf et al. (2019) also examined how the spatiotemporal organisation of lumbar and sacral motor pool activity during walking is orchestrated as a function of the slope of terrain and walking speed. These authors observed that while the overall activity of sacral motor pools decreases on negative slopes and increases on positive slopes, the lumbar motor pools increase their engagement at all slopes with regard to level walking. They suggested that the differential involvements of lumbar and sacral motor pools on slopes were related to the modifications of positive and negative COM mechanical power production. Therefore, other locomotor tasks inducing different power requirements must result in adjustments of the segmental spinal motor output. Knowledge about the adaptation of the spinal locomotor output may shed light on the modularity of neural control in normal subjects and may provide a basis for understanding deficits in patient populations (e.g., Cappellini et al. 2016; Martino et al. 2018; Wagner et al. 2018).

Another external factor that requires neuromechanical adjustments of the walking pattern is the application of constant horizontal forces that assist or hinder the progression of the subject (e.g., Asmussen and Bonde-Petersen 1974; Chang and Kram 1999; Lenzo et al. 2014; Naidu et al. 2019; Penke et al. 2019). It was observed that, as compared to unperturbed walking (i.e., without horizontal traction forces), a hindering force applied at the COM that pulls the subject backward reduces braking but increases propulsion impulse (Gottschall and Kram 2003; Conway et al. 2018), associated with a large amount of motor unit activation of lower-limb muscles (Gottschall and Kram 2003; Ellis et al. 2014). Conversely, an aiding force applied at the COM that pulls the subject forward reduces propulsion but increases braking impulse (Gottschall and Kram 2003; Penke et al. 2019). This modification of mechanical demands results in adjustments of the motor output: many muscles (e.g., gluteus maximus, vastus medialis, semitendinosus, soleus) increase their activity with a hindering traction force, whereas some muscles (e.g., vastus medialis, gluteus medius) systematically increase, and others (e.g., medial gastrocnemius, lateral gastrocnemius, soleus) decrease their activity with an aiding traction force (Gottschall and Kram 2003; Ellis et al. 2014). In addition, because the energetic cost of generating concentric (propulsive) muscle forces is more metabolically expensive per unit force than those associated with eccentric (braking) forces (Margaria 1968; Minetti et al. 1993; Chang and Kram 1999; Grabowski and Kram 2008; Dewolf and Willems 2019), the metabolic rate decreases with aiding forces and increases with hindering forces (Gottschall and Kram 2003; Zirker et al. 2013).

Based on these observations, externally applied horizontal forces have been used in clinical practice to either increase the effort required in walking by hindering the forward motion of the COM (Na et al. 2015; Wang et al. 2015) or reduce this effort by aiding the forward motion (Dionisio et al. 2018; Penke et al. 2019). In addition, the application of horizontal forces during walking can lead to changes in the neural control strategies. For example, walking with an aiding force influences the nonlinear gait dynamics (Kurz and Stergiou 2007), while a hindering force improves the gait and dynamic balance of stroke patients (Na et al. 2015). Hence, prior to extending its use in clinical practice, it is important to quantitatively estimate the effect of horizontal forces on the neuromechanical adjustment of gait.

Therefore, the purpose of this study is to analyse the modifications of the walking patterns occurring when forces that hinder or aid the forward progression of the subject are applied, with a specific focus on (1) the pendular energy exchange, (2) the phases of positive and negative power production, and (3) the related changes in the spinal locomotor output. We expect that, due to modification of the average orientation of the ground reaction force (GRF) with a constant horizontal force, the orientation of the limbs will be modified in the same direction as the GRF vector. Indeed, to limit the increase of the GRF moment arm, we hypothesised that the limb will not be anchored to the vertical but that the modification of the limb orientation will be proportional to the modification of the GRF orientation. We also expect that the imbalance between positive and negative work will reduce the pendular energy exchange of the COM during some parts of the stride. In turn, based on the documented relation between COM dynamics and the specific spatiotemporal organisation of spinal cord activity (Cappellini et al. 2010; La Scaleia et al. 2014; Dewolf et al. 2019), we also hypothesised that the activity of the sacral motor pools will decrease with an aiding traction force and increase with a hindering one, whereas the activity of the lumbar motor pools will increase at all traction levels with regard to unperturbed walking. Throughout the discussion, our results will be compared with walking on slopes (Dewolf et al. 2017, 2018, 2019) to understand if the changes in walking pattern brought on by an aiding/hindering horizontal force are similar to those brought on by vertical displacement of the COM on a negative/positive slope. Similar results would confirm that the spatiotemporal pattern of spinal cord activation might be largely determined by the power required to move the COM.

Methods

Subjects

Ten healthy subjects (age 25.6 ± 3.7 years, mass 79.7 ± 10.9 kg, height 1.80 ± 0.07 m, mean ± SD) participated in the study. Because of the fit of the harness strapped around the upper body, only males were selected. All participants gave their written informed consent. Experimental procedures were performed according to the Declaration of Helsinki and were approved by the Ethics Committee of the Université Catholique de Louvain (B403201838331).

Experimental setup and protocol

Subjects walked at three different speeds (0.83, 1.39 and 1.94 m s^{-1}) on an instrumented treadmill that consists of a modified commercial treadmill (h/p/Comos-Stellar, Germany, belt surface: 1.6 × 0.65 m, mass ~ 240 kg) measuring the fore–aft (F_f), lateral (F_l) and vertical (F_v) components of the ground reaction forces (GRF) exerted by the treadmill belt on the feet. The force signals were digitized by a 16-bit analogue-to-digital converter at 1000 Hz.

At each speed, subjects were pulled by seven different hindering/aiding horizontal traction forces F_t (± 15, ± 10, ± 5% and 0% of their body weight, BW). An upper body harness was adjusted to pull close to the geometric centre of the body (~ 57% of the subject's height, roughly at the level of the second lumbar vertebra). The harness was attached to a weight via an elastic rope and a pulley placed three metres behind/in front of the subject. This pulley was adjusted so that the rope was horizontal when the subject was standing. The pulley was equipped with a homemade force transducer measuring the horizontal traction forces, F_t. Due to friction and inertia, the traction force varied within 0.50 ± 0.54% of BW (mean ± SD) during the step (Table 1). The subject walked with a given F_t (randomised across trials) at the different speeds (randomised) before moving on to another traction percentage.

When walking at a constant speed without any traction, the average resultant force over one stride exerted on the COM is vertical (Fig. 1b). However, with a traction force, this average force deviates from the vertical and its orientation can be calculated as:

$$\beta_F = \tan^{-1}(F_t/\mathrm{BW}),$$

with $F_t = \pm 5, \pm 10$ and ± 15% BW, $\beta_F = \pm 2.86, \pm 5.71$ and ± 8.53°, respectively. These traction forces were selected so that the actual β_F was close to the inclinations of ± 3, ± 6 and ± 9° used in previous studies to analyse the effect of slope on the walking pattern (Dewolf et al. 2017, 2018, 2019).

We recorded kinematic data at 200 frames s^{-1} using a high-speed video camera (BASLER A501k, resolution 1280 × 1024 pixels, aperture time 3 ms) fixed on the ground 3 m to the side of the treadmill, perpendicular to the plane of progression. Reflective markers were placed on one side of the subject over the following landmarks: chin–neck intersect at the level of the fourth cervical vertebra, greater trochanter, lateral femoral epicondyle, lateral malleolus, heel, and fifth metatarsophalangeal joint. An additional marker was placed at a midway point between the greater trochanter

Table 1 Average F_t (±SD) throughout the trial (first line), average standard deviation of F_t (second line) and semi peak-to-peak amplitude of F_t (third line)

Speed (m s^{-1})	Theoretical level of traction in % BW (and its equivalent slope in °)					
	−15% (−8.6°)	−10% (−5.7°)	−5% (−2.9°)	5% (2.9°)	10% (5.7°)	15% (8.6°)
0.83	−14.3 ± 0.5	−9.5 ± 0.4	−4.9 ± 0.4	5.5 ± 0.6	10.2 ± 0.5	14.8 ± 0.5
	1.0 ± 0.2	0.3 ± 0.1	0.1 ± 0.1	0.1 ± 0.1	0.5 ± 0.1	1.6 ± 0.3
	1.4 ± 0.3	0.5 ± 0.1	0.2 ± 0.1	0.2 ± 0.1	0.8 ± 0.2	2.2 ± 0.4
1.39	−14.3 ± 0.5	−9.5 ± 0.3	−5.1 ± 0.4	5.2 ± 0.6	10.1 ± 0.7	14.9 ± 0.6
	1.2 ± 0.2	0.3 ± 0.1	0.1 ± 0.1	0.1 ± 0.1	0.4 ± 0.1	1.4 ± 0.2
	1.6 ± 0.4	0.5 ± 0.1	0.2 ± 0.1	0.2 ± 0.1	0.6 ± 0.3	1.9 ± 0.4
1.94	−14.5 ± 0.5	−9.6 ± 0.3	−5.0 ± 0.4	5.0 ± 0.5	9.9 ± 0.6	14.7 ± 0.5
	1.3 ± 0.2	0.3 ± 0.1	0.1 ± 0.1	0.1 ± 0.1	0.4 ± 0.1	1.2 ± 0.2
	1.8 ± 0.4	0.6 ± 0.2	0.2 ± 0.1	0.2 ± 0.1	0.6 ± 0.2	1.8 ± 0.3

All variables are expressed in % BW

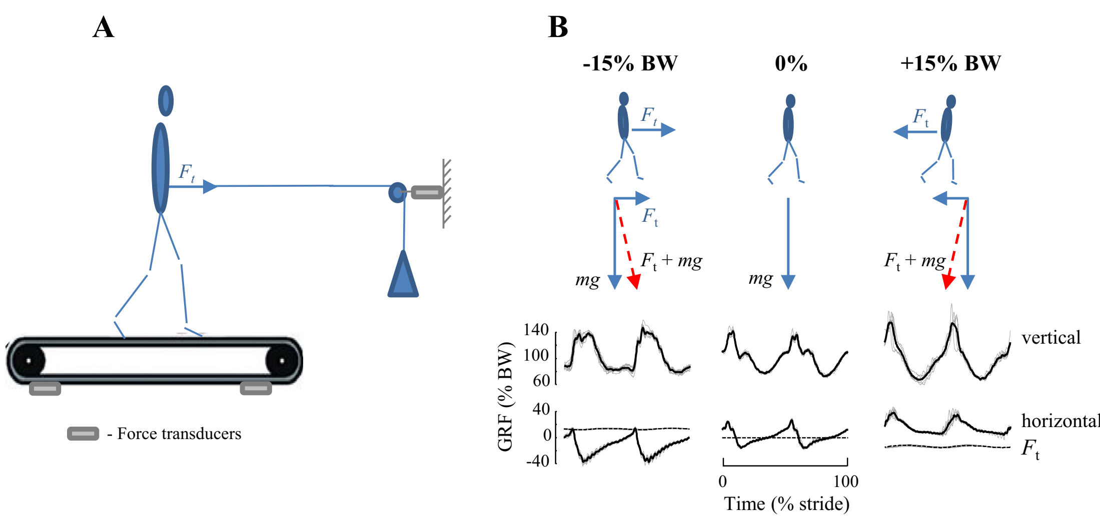

Fig. 1 **a** Schema of the experimental setup: here, the subject is walking on the instrumented treadmill with an aiding horizontal traction force. **b** Typical time traces of the resultant vertical and fore–aft ground reaction force of both legs and of the traction force F_t of one subject walking at 1.39 m s^{-1} with a −15% BW horizontal traction force (left), without horizontal traction force (middle) and with a +15% BW horizontal traction force (right). Since the lateral forces do not exceed 15% BW, they are not presented here. Grey lines represent individual traces of one subject (height 1.71 m, body mass 91.7 kg, 19.5 years) and black thick lines are the average of all the grey traces

and the lateral femoral condyle on the lateral side of the thigh, in case the hip marker was hidden by the hand. The horizontal and vertical coordinates of the reflectors in the sagittal plane were measured in each frame using Lynxzone software (Arsalis). A spline function was fitted through the experimental data to smoothen the signal and to interpolate existing points to obtain a 1000 Hz signal.

We recorded EMG activity at 1000 Hz by means of surface electrodes (wireless FREEEMG System, BTS) from 16 muscles on the right side of each subject: the erector spinae (ES) at L2 level, the gluteus maximus (Gm), the gluteus medius (Gmed), the sartorius (SART), the tensor fasciae latae (TFL), the adductor longus (ADD), the vastus medialis (VM), the vastus lateralis (VL), the rectus femoris (RF), the biceps femoris long head (BF), the semitendinosus (ST), the tibialis anterior (TA), the medial gastrocnemius (MG), the lateral gastrocnemius (LG), the soleus (SOL) and the peroneus longus (PERL). After preparing the shaved skin with alcohol, we placed EMG electrodes based on suggestions from SENIAM (seniam.org), the European project on surface EMG. To this end, we located the muscle bellies by means of palpation and oriented the electrodes along the main direction of the fibres (Winter 1991; Kendall et al. 2005). We visually inspected EMG signals during the walking trials.

Data analysis

General gait parameters

Foot contact (FC) and toe off (TO) were defined based on the displacement of the centre of pressure on the belt (Meurisse et al. 2016). The stride was defined as the period between two right FCs.

Work and power

The acceleration, velocity and the displacement of the COM were determined from the GRF using the methods of Cavagna (1975). In short, the fore–aft, lateral and vertical acceleration of the COM were, respectively, computed as $a_f = (F_f + F_t)/m$, $a_l = F_l/m$ and $a_v = (F_v\_BW)/m$, where m is the subject's body mass. The instantaneous velocity in the forward (v_f), lateral (v_l) and vertical (v_v) directions were obtained, respectively, by time integration of a_f, a_l and a_v plus an integration constant. In the fore–aft direction, this constant was chosen to make the average velocity over all the strides in a trial equal to the average velocity of the treadmill belt measured with an optical encoder v_{belt}. A stride was considered to be suitable for analysis if the sum of the increments and the sum of the decrements of v_f differed by less than 25%. In the two other directions, constants were chosen to make the average vertical and lateral velocity over each stride equal to zero. A second integration of the vertical velocity yielded to the vertical displacement of the COM (h). The kinetic energy of the COM, E_k, was calculated as the sum of E_{kf}, the kinetic energy due to the forward movements of the COM, E_{kl} the kinetic energy due to its lateral movements and E_{kv} the kinetic energy due to its vertical movements. Since the traction exerted a constant horizontal force F_t, similar to the field of force exerted by gravity in the vertical direction, we considered F_t as a second force field exerted horizontally on the subject and the 'potential' energy of the system (E_p^*) relative to these force fields was calculated as:

$$E_p^* = \mathrm{mgh} + W_t,$$

where W_t is the work done by the traction force computed as:

$$W_t = \int F_t v_{belt} dt.$$

The work done by the subject to sustain the motion of the COM (W_{ext}) can thus be calculated as:

$$W_{ext} = E_k + E_p^*.$$

Positive (W_{ext}^+) and negative (W_{ext}^-) COM work were computed by summing the increments and the absolute value of the decrements of the W_{ext} curve, respectively. The COM power, $\dot{W}_{ext}$, can be computed by:

$$\dot{W}_{ext} = dW_{ext}/dt.$$

The pattern of fluctuation of $\dot{W}_{ext}$ during unperturbed walking typically presents one major peak of negative power ($\dot{W}^-$) and two major peaks of positive power: $\dot{W}_1^+$ and $\dot{W}_2^+$ (Cavagna et al. 1976). Here, the maximum of each of these three peaks was measured across all conditions.

Recovery and pendular energy savings within the step

To identify periods within each step during which an energy transduction between kinetic and potential energy occurs (like in a pendulum), the within-step recovery at each instant t of the step [$r(t)$ in %] was measured as in Cavagna et al. (2002):

$$r(t) = 100 \frac{\left|E_k(t) - E_k(t - \Delta t)\right| + \left|E_p^*(t) - E_p^*(t - \Delta t)\right| - \left|W_{ext}(t) - W_{ext}(t - \Delta t)\right|}{\left|E_k(t) - E_k(t - \Delta t)\right| + \left|E_p^*(t) - E_p^*(t - \Delta t)\right|}$$

where Δt is the time between two samples.

To evaluate the theoretical amount of mechanical power saved by this recovery, the theoretical rate of 'pendular energy savings', $\dot{e}(t)$ was computed as in Dewolf et al. (2017):

$$\dot{e}(t) = \frac{\left|E_k(t) - E_k(t - \Delta t)\right| + \left|E_p^*(t) - E_p^*(t - \Delta t)\right| - \left|W_{ext}(t) - W_{ext}(t - \Delta t)\right|}{\Delta t}.$$

Typical $r(t)$ and $\dot{e}(t)$ curves are presented in Fig. 3. Four periods (T1–T4) were defined according to the local maxima and minima of E_k and E_p^*: the first period T1 occurs when E_p^* increases while E_k decreases; a subsequent period T3 occurs when E_p^* decreases while E_k increases; between T1 and T3 and between T3 and T1, we define the period T2 and T4, respectively, where E_p^* and E_k changes are in phase. E_s was defined as the time integral of $\dot{e}(t)$ over each period.

Orientation of the body segments

From the marker locations, the hip, knee and ankle joint angles and the average trunk orientation (i.e., the orientation of the line joining chin–neck intersect and greater trochanter) relative to the vertical axis were computed. During stance, the contact moves from the heel to the front foot as stance progresses from FC to TO. The actual limb orientation was approximated from the markers of the greater trochanter and the heel at FC and from the markers of the greater trochanter and the fifth metatarsophalangeal joint at TO (Fuchioka et al. 2015). At FC and TO, the angle relative to vertical was measured.

EMG activity and spinal maps

The raw EMG signals were high-pass filtered (30 Hz), then rectified and low-pass filtered with a zero-lag third-order Butterworth filter (10 Hz), to obtain the EMG envelopes. To reduce residual baseline noise, the minimum signal from each envelope was subtracted (La Scaleia et al. 2014; Cappellini et al. 2016). For each subject and for each condition, the average EMG activity was calculated across all gait cycles.

Because the spatiotemporal patterns of the spinal motor output of slope walking have been considered bilaterally (Dewolf et al. 2019), we applied similar methods here. The rationale for the bilateral analysis is that the COM motion results from muscle activities of both legs rather than activities of only one leg. To obtain an estimate of the EMG activity of the left side of the subjects, right average EMG activity were half-cycle shifted, assuming symmetry of bilateral activations (Pierotti et al. 1991; Burnett et al. 2011). The activity of the left and right leg muscles was then collapsed within one gait cycle defined for the right leg. The EMG signal from each of the 32 muscles (i.e., 16 measured on right side and 16 projected to estimate left side) was then normalised to its peak value across all conditions for each participant. The bilateral average EMG activities were then mapped onto the estimated rostrocaudal location of the MN pools in the human spinal cord from the L2 to S2 segments based on Kendall's myotomal charts as in Ivanenko et al. (2006, 2013). To account for size differences in MN pools at each spinal level, this fractional activity value was then multiplied by the segment-specific number of MNs (MN_j), taken from Tomlinson and Irving (1977).

To compute the relative activation of the lumbar and sacral segments in each walking condition, we averaged the motor output patterns over the gait cycle in the upper part of the lumbar (sum of the activity from L2 to L4) and the sacral segments (sum of activity from S1 to S2). To reduce overlaps due to maps smoothing, the spinal segment L5 was not taken into account.

Statistics

The statistical analysis was designed to assess the effect of walking speed, of the horizontal traction force and of the interaction between these two factors. A two-level linear mixed model was applied with post hoc Bonferroni correction (PASW Statistics 19, SPSS inc®, IBM company, USA): speed and traction were set as fixed effects, and the subject was set as a random effect. The normality of the residuals was checked by the Kolmogorov–Smirnov. An α threshold of 0.05 was used throughout to assess statistical significance.

Results

Gait and kinematic parameters

The stride period (Fig. 2a) decreases with speed ($F_{2,209}=505.4$; $p<0.001$) and is significantly affected by the horizontal traction force ($F_{6,209}=25.7$; $p<0.001$): as compared to unperturbed walking, the stride period decreases when walking with an aiding traction force of −15 and −10% of BW ($p<0.001$). However, the effect of this aiding force is reduced as speed increases (interaction: $F_{12,209}=4.6$; $p<0.001$). The relative duration of the swing phase is not affected by either the walking speed or by the horizontal traction force, except with a −15% aiding force, where it is slightly greater than during unperturbed walking ($p=0.005$).

Figure 2b shows the average waveforms of lower-limb joint angles at 1.39 m s^{-1} during unperturbed walking and with a traction of ± 15%. As compared to unperturbed walking, the major kinematic changes with a 15% hindering force occurring at FC, where the hip, knee and ankle joint are more flexed (hip, knee and ankle: $p<0.001$). With an aiding force, the major kinematic modifications are a decrease of hip extension ($p=0.001$) and an increase of knee flexion ($p<0.001$) during stance phase. The modification of hip joint angle is partly due to the fact that the average orientation of the trunk is affected by both the horizontal traction force ($F_{6,209}=123.9$, $p<0.001$) and speed ($F_{2,209}=27.8$, $p<0.001$) (Fig. 2c). The body bends forwards with increasing speed as compared to unperturbed walking, the trunk shows a forward tilt with increasing hindering forces and a backward tilt with aiding forces.

As compared to unperturbed walking, the limb angle at FC (approximated from the markers of the greater trochanter and the heel) decreases with a hindering force ($p<0.01$), whereas it does not change with an aiding force ($p>0.485$). The limb angle at TO (approximated from the markers of the greater trochanter and the fifth

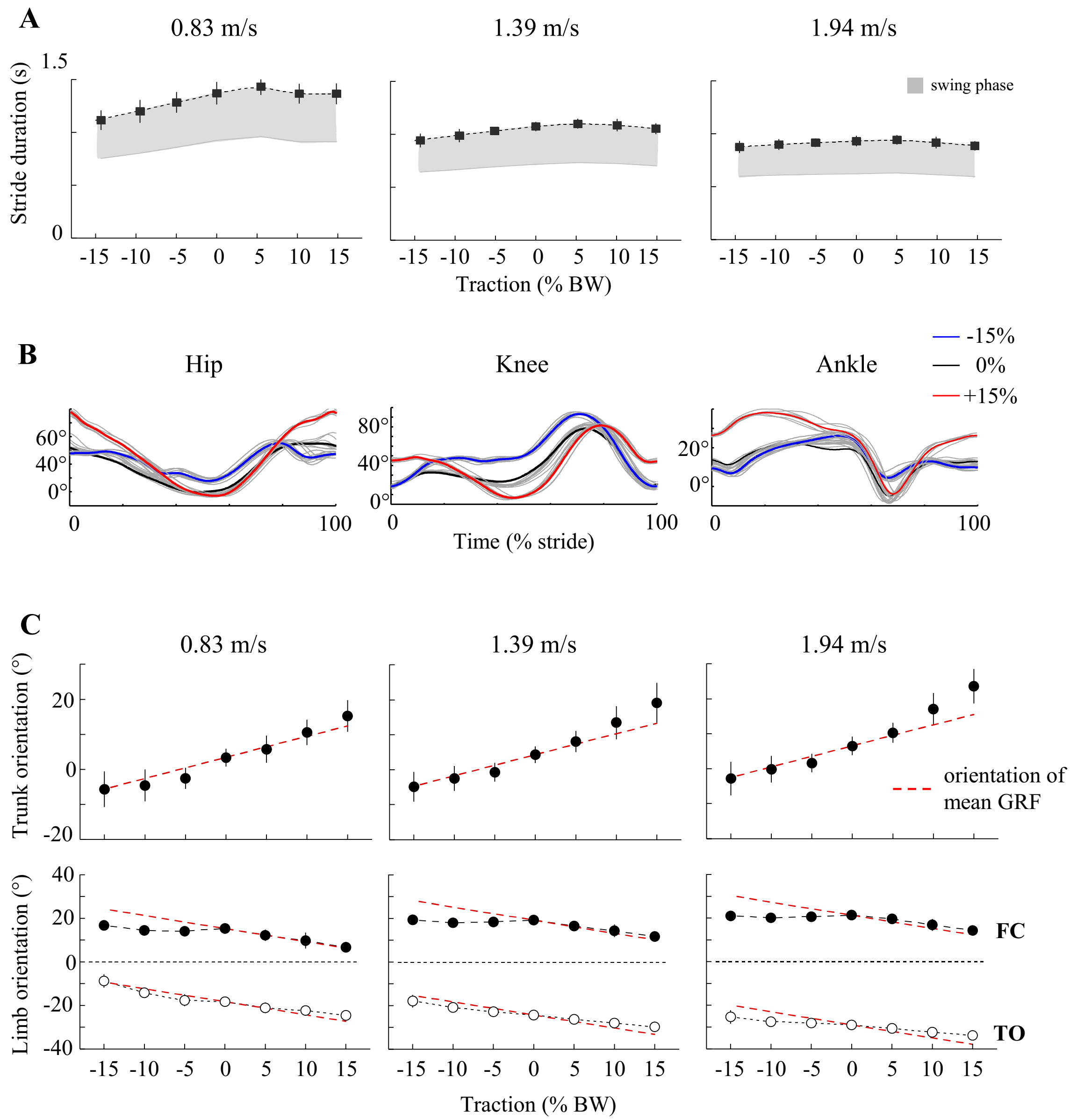

Fig. 2 **a** Stride period (squares), divided into swing phase (grey area) and stance phase as a function of the horizontal traction force. **b** Hip (left), knee (middle), and ankle (right) joint angles over a stride during walking at ~ 1.39 m s^{-1} with different levels of horizontal traction force (− 15%, 0% and 15% BW). The colour and grey curves represent the average (across strides) and individual strides of one subject (same as in Fig. 1), respectively. Zero percent and 100% correspond to the right foot contact. **c** Average orientation of the trunk (top) and orientation of the limb relative to vertical at foot contact (FC; black circles) and toe off (TO; open circles) (bottom) as a function of horizontal traction force at 0.83 (left), 1.39 (middle), and 1.94 m s^{-1} (right). The red dotted lines correspond to the orientation of the average ground reaction force. In **a** and **c**, symbols and bars represent the grand means and SDs of all subjects (SDs are presented only when the length of the bar exceeds the size of the symbol). The continuous lines were drawn through experimental data using a weighted mean function (KaleidaGraph 4.5; Synergy Software, USA)

metatarsophalangeal joint) is also affected by the traction force ($F_{6,209} = 98.7$, $p < 0.001$): it decreases with aiding forces, whereas it increases with hindering forces. At all traction forces, both the limb angle at FC ($F_{6,209} = 152.2$, $p < 0.001$) and the limb angle at TO ($F_{6,209} = 514.0$, $p < 0.001$) increase when speed becomes faster, because stride length increases. Note that, except for the limb angle at FC with aiding forces, the change in orientation of the limb corresponds approximately to the change in the orientation of the average GRF.

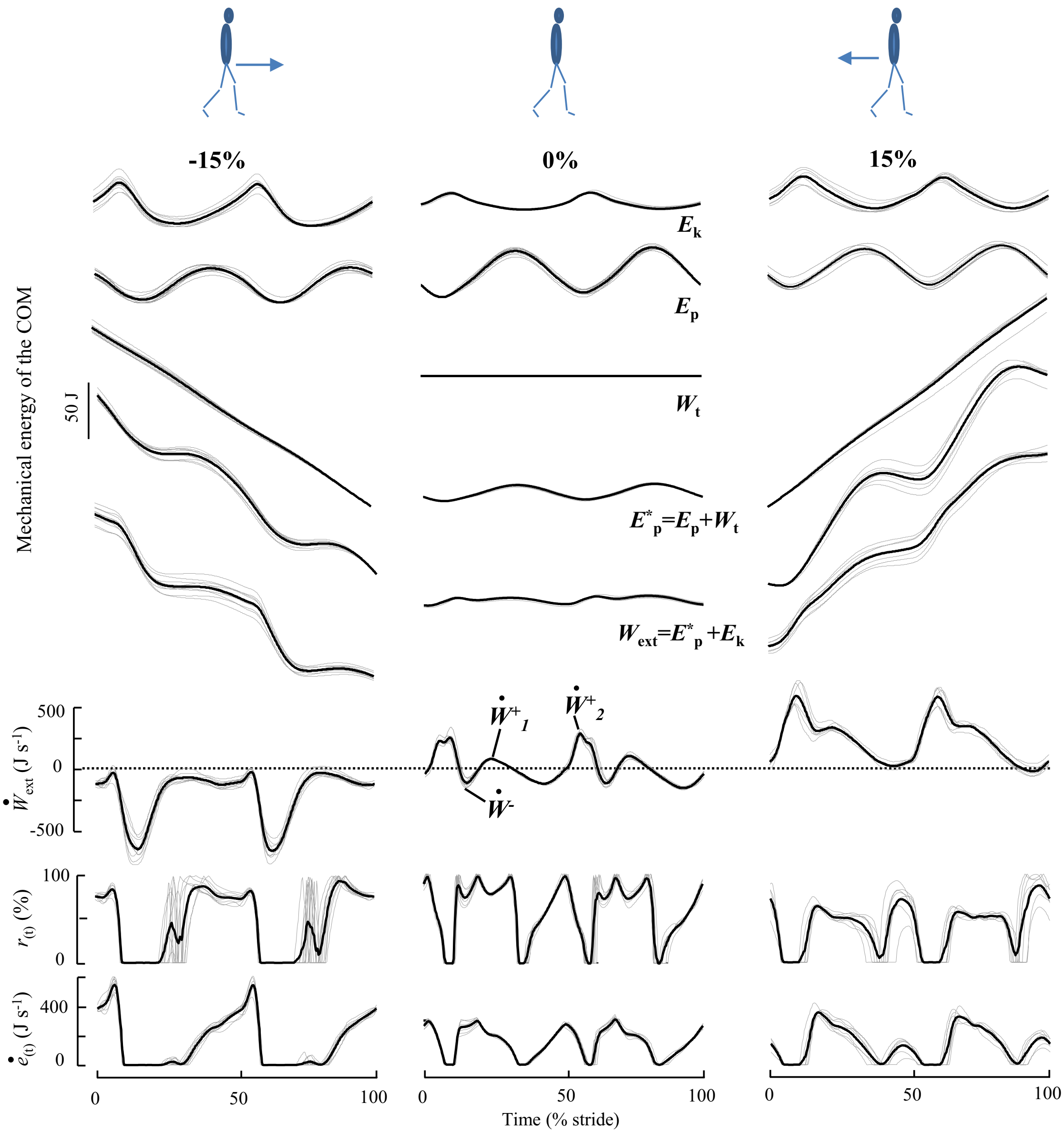

Fig. 3 Typical traces over a stride from a subject walking at ~ 1.39 m s^{-1} with a −15% BW horizontal traction force (left), without horizontal traction force (middle) and with a +15% BW horizontal traction force (right). Top panels: Mechanical energy–time curves of the COM: from top to bottom, the first curves (E_k) refers to the kinetic energy of the COM, the second curves to its gravitational potential energy ($E_p = mgh$), the third curve (W_t) to the work done by the traction force, the fourth curve (E^*_p) to its potential energy (calculated as $E^*_p = mgh + W_t$) and the last curve ($W_{ext} = E_k + E^*_p$) to the work done by the subject to move the COM. Bottom panels: power developed by the subject to move the COM, instantaneous recovery *r(t)* and rate of pendular energy savings *e(t)* at each instant of the stride. Time is expressed as a percentage of the stride period. Grey lines represent individual traces of one subject (same as in Fig. 1) and black thick lines are the average of all the grey traces

Pendular energy exchange within the step

Figure 3 presents typical traces of E_k, E^*_p, W_t , W_{ext}, $\dot{W}_{ext}$, $r(t)$ and $\dot{e}(t)$ during a walking stride at 1.39 m s^{-1}. As compared to unperturbed walking, to counteract the work done by the traction forces, E^*_p increases with a hindering force ($F_{6,209} = 653.6$, $p < 0.001$), while E^*_p decreases with an aiding force ($F_{6,209} = 627.8$, $p < 0.001$). This difference with a traction force causes an imbalance between W^+_{ext} and W^-_{ext} and affects the transduction of E_k into E^*_p during T1 ($F_{6,209} = 1014.3$, $p < 0.001$) and of E^*_p into E_k during T3 ($F_{6,209} = 55.2$, $p < 0.001$).

When walking with traction, the duration of the different phases changes as compared to unperturbed walking

Fig. 4 **a** Duration of the phases during which the pendulum-like energy transduction occurs during a stride of walking at ~ 1.39 m s^{-1}, as a function of traction level (y axis). The time is expressed as a percentage of the step duration: 0% and 100% correspond to right FC. Closed circles correspond to the instant of $E_{k,max}$, open circles to $E_{k,min}$, closed squares to $E^{*}_{p,max}$, and open squares to $E^{*}_{p,max}$. The grey zones correspond to the phases during which E_k can be transformed into E_p (T1) and vice versa (T3). The white zones correspond to the phases during which the curves are in phase. **b** Duration (in % of stride; top) and pendular energy savings (E_s in J kg^{-1}; bottom) over the periods T1 (left) and T3 (right) as a function of traction level at each speed. Symbols represent the grand mean of all subjects at a given traction and bars represent the SDs (when the length of the bar exceeds the size of the symbol)

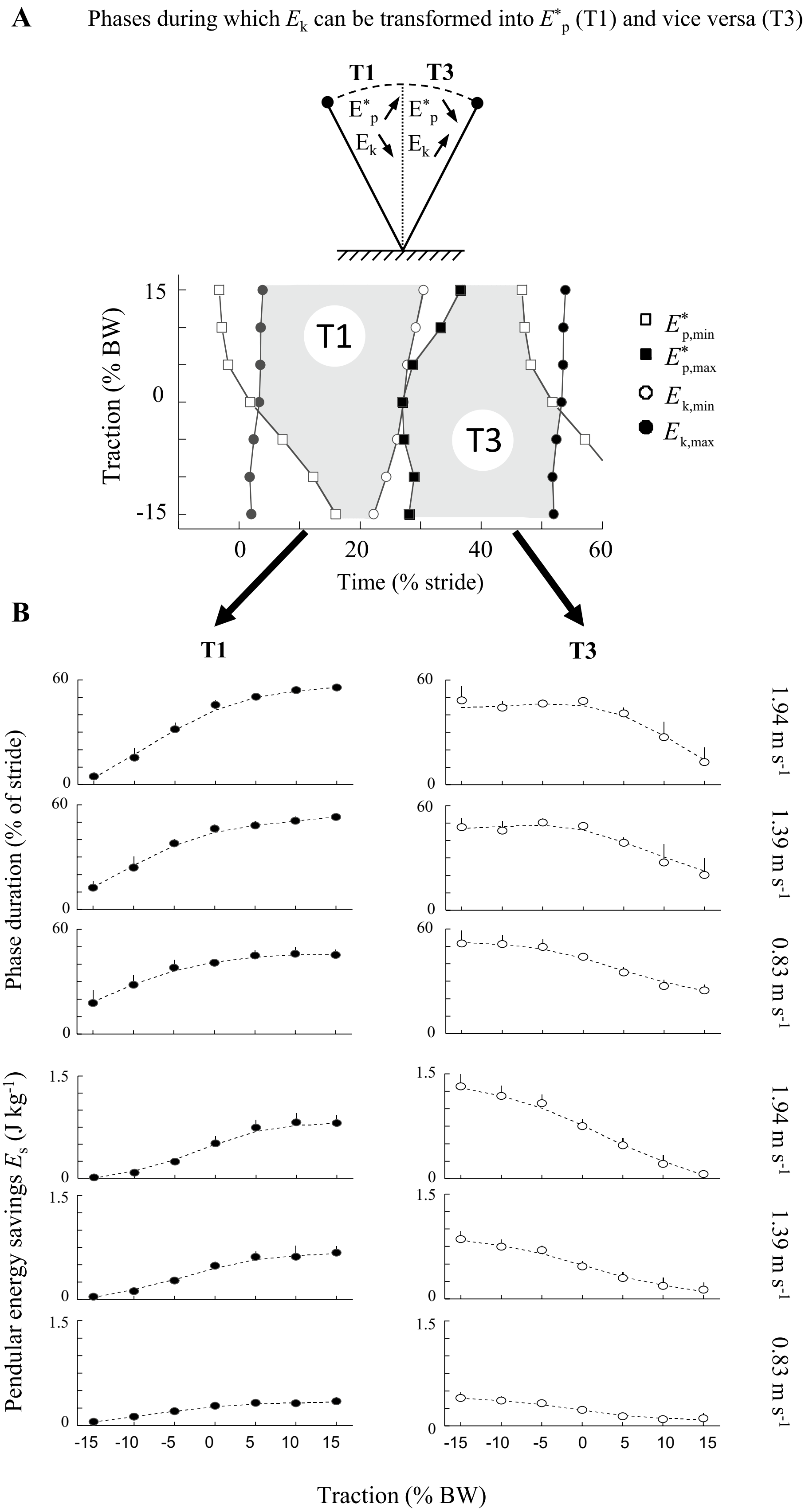

(Fig. 4). While the duration of T1 and T3 and E_s during T1 and T3 are about equal at all speeds during unperturbed walking (Cavagna et al. 2002; Dewolf et al. 2017), T1 becomes shorter ($p < 0.001$), while T3 does not change significantly with aiding traction forces (Fig. 3). In addition, during T1 E_s becomes on average more than ten times smaller ($p < 0.001$) and during T3 E_s becomes on average two times greater ($p < 0.001$) than during unperturbed walking. With hindering forces, as compared to unperturbed walking, T3 becomes relatively shorter ($p < 0.001$) and during T3 E_s becomes smaller ($p < 0.001$), while T1 becomes relatively longer ($p < 0.001$) and during T1 E_s becomes greater ($p < 0.001$). All effects are more pronounced when walking at higher speeds (interaction, $F_{12,209} > 5.1$, $p < 0.001$).

Modification of power requirement

When walking with or without aiding traction forces, the $\dot{W}_{ext}$ time curves display one peak of negative power ($\dot{W}^-$) occurring ~ 10% after FC (Fig. 3). At low walking speeds, the magnitude of this peak is slightly greater when walking with aiding forces. When speed increases, the magnitude of this peak increases ($F_{2,209} = 639.1$, $p < 0.001$) at a faster rate with an aiding force than during unperturbed walking (interaction: $F_{12,209} = 128{,}5$, $p < 0.001$).

During unperturbed walking, the $\dot{W}_{ext}$ time curves display two peaks of positive power. The magnitude of these two peaks increases with speed ($\dot{W}_1^+$: $F_{2,209} = 355.4$, $p < 0.001$ and $\dot{W}_2^+$: $F_{2,209} = 136.7$, $p < 0.001$) and with hindering traction forces ($\dot{W}_1^+$: $F_{6,209} = 102.7$, $p < 0.001$ and $\dot{W}_2^+$: $F_{6,209} = 377.1$, $p < 0.001$. When walking with an aiding force, both $\dot{W}_1^+$ and $\dot{W}_2^+$ decreases with increasing traction force

EMG activities and spinal motor output

Figure 5a illustrates typical traces of the EMG envelopes when walking at 1.39 m s^{-1} with traction of − 15, 0 and 15% of BW. As compared to unperturbed walking, the EMG amplitude of many muscles increases with a + 15% hindering traction (TFL, ADD, VM, VL, RF, MG, LG, SOL and PERL: $p \leq 0.001$), whereas with a − 15% aiding traction, the amplitude of some EMGs reduces (MG and PERL: $p \leq 0.001$), while the amplitude of other EMGs increases (RF: $p = 0.004$, VM: $p < 0.001$) (Ellis et al. 2014). We also observe some deviations from the EMG bursting patterns observed during unperturbed walking. Indeed, an additional burst of activity appears in ST and BF at the end of stance with a hindering force and in ES at the onset of stance with an aiding force.

Figure 5b presents the EMG of Fig. 5a mapped onto the estimated rostrocaudal location of the MN pools in the spinal cord. Two major spots of activity are present and their mean motor output intensities increase with speed ($F_{2,209} > 371.19$, $p < 0.001$): the first burst occurs around foot contact and is mainly localised at the lumbar segment, while the second burst occurs during the second part of single stance and is mainly localised at the sacral segment (Ivanenko et al. 2006, 2013b; Cappellini et al. 2010). The most striking result is that the intensity of these two spots is differently affected by hindering and aiding traction forces: as compared to unperturbed walking, the maximal intensity of the major lumbar MN activation increases with both hindering and aiding traction forces ($F_{6,209} > 97.8$, $p < 0.001$), whereas the maximal intensity of the sacral MN activation increases with hindering traction forces ($p < 0.001$) and reaches a minimum at a traction of − 10% BW (Fig. 6).

Discussion

The present study is intended to analyse modification of gait when a constant aiding or hindering horizontal force is applied. To this end, we assess the changes of limb kinematics, COM dynamics and the related spatiotemporal organisation of motor pool activity in the spinal cord. In particular, our results reveal that the trunk and limb axis orientations are tilted as compared to unperturbed walking and that the angle of these tilts approximatively corresponds to the modification of the orientation of the average GRF (Fig. 2c). As first indicated by di Prampero et al. (2005), our results confirm that the angle between the line joining the point of foot contact–ground with the COM and the ground is equivalent when walking on a certain percentage of slope or when walking with a theoretically equivalent traction force. Therefore, other locomotor tasks inducing different power requirements must result in adjustments of the segmental spinal motor output. Knowledge about the adaptation of the spinal locomotor output may shed light on the modularity of neural control in normal subjects and may provide a basis for understanding deficits in patient populations (e.g., Cappellini et al. 2016; Martino et al. 2018; Wagner et al. 2018).

Similarities of COM dynamics between walking with a horizontal traction force and on an equivalent slope

When walking with a hindering traction force, the increase in W_{ext}^+ to counteract this force is accompanied by a decrease in W_{ext}^-. Conversely, when walking with an aiding force, the increase in W_{ext}^- is accompanied by a reduction of W_{ext}^+. These

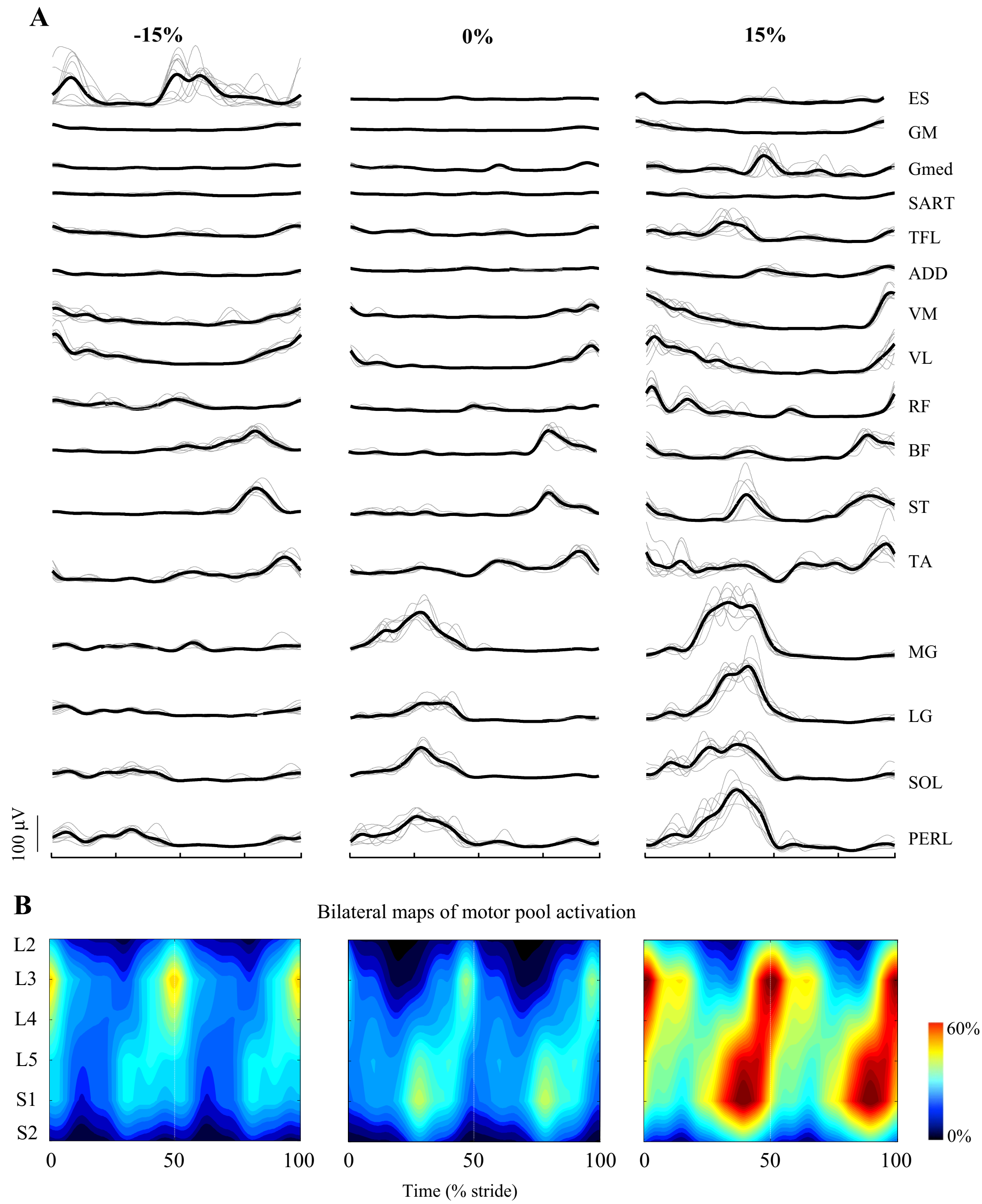

Fig. 5 **a** EMG patterns of 16 lower-limb muscles during walking at ~1.39 m s^{-1} with a −15% BW horizontal traction force (left), without horizontal traction force (middle) and with a +15% BW horizontal traction force (right). The time is expressed as a percentage of the step duration: 0% and 100% correspond to right FC. *ES* erector spinae, *GM* gluteus maximus, *Gmed*, gluteus medius, *SART* sartorius, *TFL* tensor fascia latae, *ADDL* adductor longus, *VM* vastus medialis, *VL* vastus lateralis, *RF* rectus femoris, *BF* biceps femoris, *ST* semi tendinous, *TA* tibialis anterior, *GM* gastrocnemius medialis, *LG* lateral gastrocnemius, *SOL* soleus, *PERL* peroneus longus. Grey lines represent individual traces of one subject (same as in Fig. 1) and black thick lines are the average of all the grey traces. **b** Bilateral spatiotemporal spinal motor outputs computed from the EMGs of Fig. 5a. Motor output (reported in % of maximal activation during the stride; 100% would correspond to a maximal activation of the 16 muscles at the same time) is plotted as a function of gait cycle. Colours change in function of the activity level (see scale at the right side of the panel)

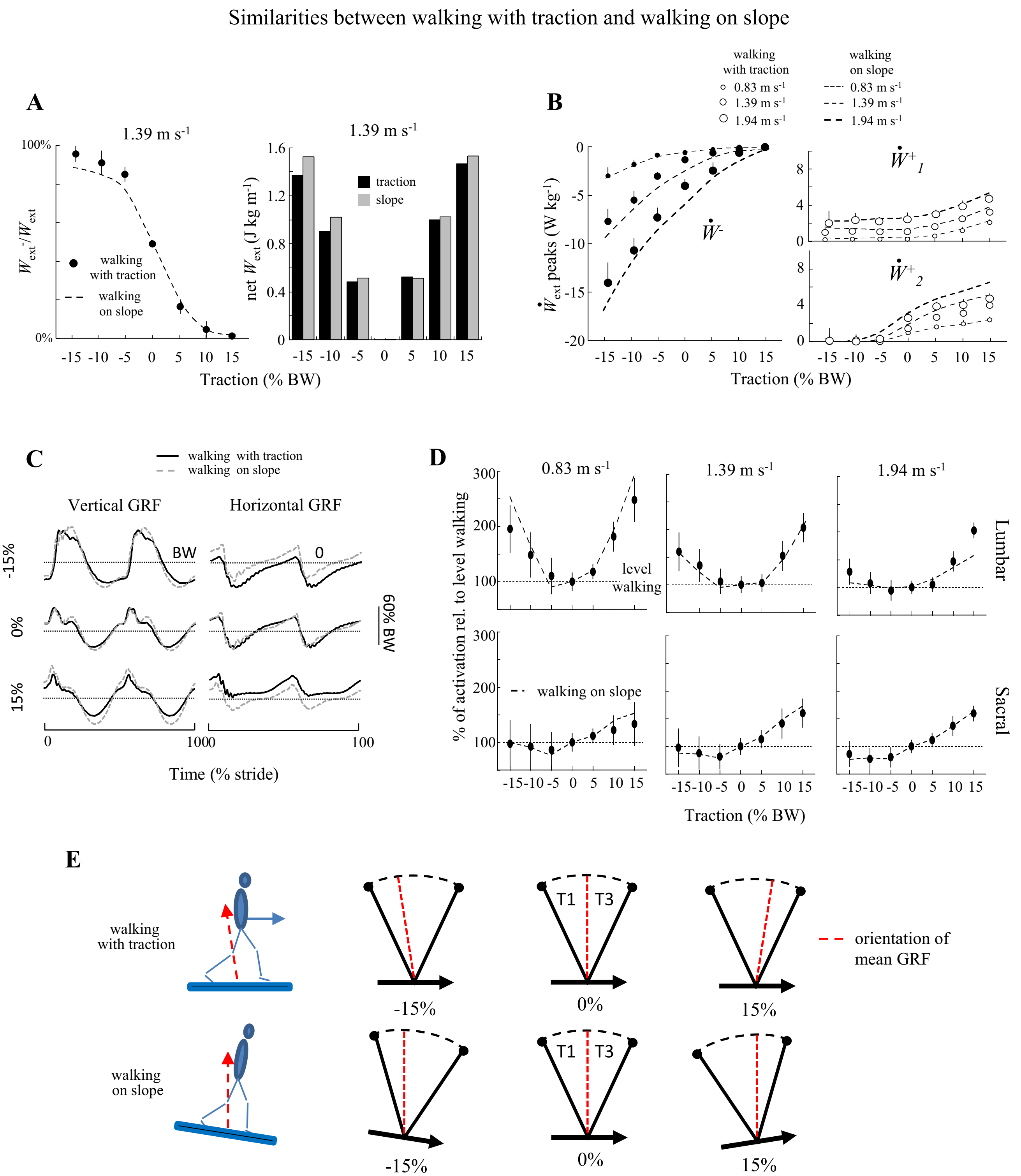

modifications are similar to those observed during walking on an equivalent slope (Fig. 6), except that W^{+}_{ext} is slightly lower with an aiding force than during walking on an equivalent slope. Despite these small discrepancies, the difference between W^{+}_{ext} and W^{-}_{ext}, which represents the net W_{ext} done by the subject over the stride and which is exactly equal to W_{t}, is similar with a traction force or with an equivalent slope (di Prampero et al. 2005). Indeed, as first argued by these authors, our results confirm that the net W_{ext} can be computed as:

$$\text{net } W_{\text{ext}} = mgL \sin \beta_{\text{F}}$$

◂**Fig. 6** **a** Left: percentage of negative work done by the GRF relative to the total work done when walking at ~ 1.39 m s^{-1} as a function of traction level. The interrupted line corresponds to the data obtained on equivalent slopes. Right: net work done by the subject during walking at ~ 1.39 m s^{-1} as a function of traction level (black bars). The grey bars correspond to the data obtained on equivalent slopes. Bars are the grand mean of all subjects at a given traction/slope. **b** Changes in the positive ($\dot{W}_1^+$ and $\dot{W}_2^+$) and negative ($\dot{W}^-$) peaks of the power done by the ground reaction force with speed and traction level. The interrupted lines correspond to the data obtained on equivalent slopes. The thickness of the lines and the size of the symbols increase with increasing speed. **c** Ensemble average of the vertical (left) and horizontal (right) ground reaction force over a stride during walking at ~ 1.39 m s^{-1} with a − 15% BW horizontal traction force (top), without horizontal traction force (middle) and with a + 15% BW horizontal traction force (bottom). Black lines correspond to walking with a traction force, whereas interrupted grey lines correspond to walking on an equivalent slope. **d** Changes in the mean intensity of the estimated upper lumbar (L2 + L3 + L4) and sacral (S1 + S2) segments with walking speed and traction level, expressed as the percentage of activity measured without traction force. The interrupted line corresponds to the data obtained on equivalent slopes. **e** Schematic representation of changes in the arched COM trajectory relative to the ground with the two phases of pendular energy exchange (T1 and T3) and to the orientation of the average ground reaction force during walking with a traction force (top) or on a slope (bottom). In each panel, symbols represent the grand mean of all subjects at a given traction and bars are the standard deviations (when the length of the bar exceeds the size of the symbol)

where β_F is either the average orientation of the GRF relative to the vertical or the inclination of the terrain. Note that the small differences observed in net W_{ext} are due to the fact that the applied horizontal traction forces are slightly smaller than 5, 10 and 15% of BW (see Table 1).

During unperturbed walking (i.e., without horizontal traction force), the arched trajectory of the COM, described at first approximation by a 'compass gait model', is more or less symmetric with respect to the vertical (Saunders et al. 1953; Alexander 1995; Usherwood et al. 2008). To illustrate how and why the E_k–E_p^* transduction is modified when walking on a slope, Dewolf et al. (2017) tilted the arc of the compass gait model backward in uphill walking and forward in downhill walking, to maintain the arched trajectory of the COM more or less symmetric with respect to the normal to the surface (see schemas in Fig. 6e). When walking with a horizontal traction force, the position of the hip relative to the foot at foot contact (FC) and toe off (TO) and the trunk orientation are tilted relative to unperturbed walking (Fig. 2c). Relative to the vertical, the trailing limb angle increases while the leading limb angle decreases with a hindering traction force, which may be done to increase the magnitude of propulsive force generation (Hsiao et al. 2015; Naidu et al. 2019). The contrary may be observed with an aiding traction force, most likely to increase braking force generation. However, it is worth stressing that the adaptation of the COM trajectory cannot be accounted for by a simple tilt such as on a slope. Indeed, because the net vertical displacement of the COM over a stride must be nil on flat ground, the modification of limb angle must be compensated by a change in limb length to maintain the arched trajectory of the COM centred on the vertical. However, since the average orientation of the GRF is no longer vertical when walking with a horizontal traction force, the arched trajectory of the COM becomes asymmetric with respect to the adapted GRF orientation (Fig. 6e). As a consequence, compared to unperturbed walking, the duration of T1 and E_s becomes greater with positive tractions (or slopes), whereas the duration of T3 and E_s becomes greater in negative tractions—or slopes (Figs. 3 and 4). The asymmetry between T1 and T3 increases with walking speed (Dewolf et al. 2017, Fig. 4).

Whilst walking on a slope, the power required to move the COM ($\dot{W}_{ext}$) accounts for most of the differences in the energetics of walking on slopes (Minetti et al. 1993; Dewolf et al. 2019). Here, we observed that the requirements for maintaining walking speed with horizontal traction force result in an increased propulsion or braking generation, without altering vertical limb loading (Naidu et al. 2019, Fig. 6c). Despite the different requirement for raising/lowering and accelerating/decelerating the COM during walking with traction as compared to walking on slopes, similarities between the vertical and horizontal GRF and the $\dot{W}_{ext}$ are striking (Fig. 6b, c; Dionisio et al. 2018). Even if the average vertical velocity of the COM is not nil when walking on slopes whereas the average horizontal GRF is not nil when walking with traction, the modifications of $\dot{W}_{ext}$ resemble those observed during walking on slopes.

Adjustments of the spinal motor pool activation when walking with a hindering or aiding traction force

It has been recently reported that the modification in COM dynamics of walking is related to specific spatiotemporal organisation of motor pool activity in the spinal cord (Cappellini et al. 2010; La Scaleia et al. 2014; Dewolf et al. 2019). Indeed, when mapping multi-muscle EMG activity onto the rostrocaudal location of the motoneuron pools, the net spinal motor output exhibits bursts of activity around foot lift off of the trailing limb and touchdown of the leading limb (Ivanenko et al. 2006, 2013b; La Scaleia et al. 2014; Maclellan et al. 2014) that contributes to raising/lowering and accelerating/decelerating the COM (Fig. 5). The substantial reorganisation of spinal locomotor networks observed when walking with a traction force corroborates the specialisation of neuronal networks located at different segments of the spinal cord for performing specific locomotor tasks. When walking with a horizontal traction force, the most striking feature in the spinal maps is the differential involvements of the lumbar and sacral motor pools (Fig. 6d), associated with a systematic temporal correspondence between the major loci of spinal motor output and the fluctuations of $\dot{W}_{ext}$. In brief, the sacral spinal activity and the second peak of positive power ($\dot{W}_2^+$) commence before foot contact and their magnitude increases with horizontal traction force from − 15 to + 15% of BW (Fig. 6b, d). The changes in sacral spinal activity and in $\dot{W}_2^+$ correspond to the decrease/increase in the distal extensor muscles activity with an aiding/hindering traction force (Fig. 5a; Gottschall and Kram 2003; Ellis et al. 2014; Dionisio et al. 2018). The lumbar spinal activity is associated with a peak of negative power $\dot{W}^-$ followed by the first peak of positive power $\dot{W}_1^+$, occurring after foot contact. When walking with a hindering traction force, the lumbar spinal activity increases and is associated with an increase in $\dot{W}_1^+$ whereas with an aiding traction force, the lumbar spinal activity increases and is associated with an increase in $\dot{W}^-$. These changes correspond to the increase in proximal extensor muscles activity with an aiding/hindering traction force (Fig. 5a; Ellis et al. 2014).

By analysing both biomechanical and neurophysiological aspects of gait, our findings point toward the relationship between the adaptability of the segmental spinal motor output due to external constraints and the COM power during terrestrial locomotion. Previous studies have experimented the use of externally applied horizontal forces in clinical practice (Na et al. 2015; Wang et al. 2015; Dionisio et al. 2018; Penke et al. 2019) to either increase or reduce the effort to walk, that was evaluated based on the modification of oxygen consumption (Gottschall and Kram 2003), or to change the orientation of the trunk when a backward tilt is induced by the application of an upward 'gravity-assisting' forces (Mignardot et al. 2017). However, neuromechanical adjustments of gait have been rarely detailed. Knowledge about the dependence of spatiotemporal patterns of spinal cord activations on COM dynamics may have important clinical implications. For example, stimulation techniques of the spinal cord segment seem to be a promising tool to restore the functioning of the spinal pattern generation circuitry (Solopova et al. 2017; Gill et al. 2018; Wagner et al. 2018; Sayenko et al. 2019). Understanding the functional organisation of the spinal locomotor output with different biomechanical requirements (Ivanenko et al. 2008; Cappellini et al. 2010, 2016; Chvatal et al. 2011) may lead to selective stimulation of the lumbar and sacral segment of the spinal cord, depending on walking conditions. The application of horizontal traction forces could also be used as a tool to assess or train propulsion or braking capability. Future rehabilitation interventions may be able to provide adaptation when applying horizontal forces to restore gait dynamics, for example, during partial body weight-supported gait therapy (Mignardot et al. 2017). Such controlled horizontal forces would affect the repartition of muscle efforts (Fig. 5) and the energetic cost of walking (Simha et al. 2019; Penke et al. 2019) and should be adapted to challenge individual walking abilities during rehabilitation.

This study has some limitations inherent to the methods and protocol used. First, the instrumented treadmill used in this study does not allow measuring individual limb GRFs. Therefore, a comparative analysis of individual lower-limb joint powers was not possible. Second, while the hindering or aiding external forces applied to the subject were assumed constant, the instantaneous force F_t slightly fluctuated during the stride (Fig. 1b and Table 1) due to the periodic nature of walking (Bhat et al. 2019). As such, a non-constant force profile may slightly affect our results since the timing of horizontal forces applied to the COM significantly affect the energetic cost of walking (Penke et al. 2019). Third, some implicit assumptions are made to reconstruct the spinal motor output from multi-muscle EMG recordings, detailed in Ivanenko et al. (2013). In particular, the EMG activity of the left side of the subjects was estimated assuming a perfect symmetry with their right side, to simplify data collection and analysis. However, asymmetrical muscle activities may reflect individual differences between the limbs (Sadeghi et al. 2000). Due to the relatively small cohort, the effect of traction force and speed was not assessed on an individual basis; an individual's characteristics—such as leg length or physical capability—are likely to affect the walking pattern, especially at the fastest speeds, which is close to the spontaneous walk-to-run transition.

Despite these limitations, by analysing both the biomechanical and the neurophysiological aspects of gait, in addition to the corresponding modifications of mechanical requirements (Fig. 6a–c), our findings point toward a similar reorganisation of the spinal locomotor networks when walking with a horizontal traction force or on an equivalent slope (Fig. 6d). While similarities between horizontal traction forces and equivalent slopes has already been documented during running (Chang and Kram 1999; Avogadro et al. 2004; Gimenez et al. 2014), the present study is the first to demonstrate kinematic, COM dynamics and EMG similarities during walking gait. In turn, since tilting instrumented treadmills is challenging, our results suggest that horizontal traction forces may also be used to simulate slope locomotion in laboratories that do not have appropriate measurement devices.

Acknowledgements This work was supported by the Italian Ministry of Health (Ricerca corrente, IRCCS Fondazione Santa Lucia), Italian Space Agency (Grants I/006/06/0 and 2019-11-U.0), Italian University Ministry (PRIN Grants 2015HFWRYY_002 and 2017CBF8NJ_005).

Author contributions PAW and AHD: conceptualization. AHD and RMM: data curation. AHD: formal analysis. FL and PAW: funding acquisition. AHD and YPI: investigation. AHD, YPI and RMM:

methodology. FL and PAW: project administration. AHD: software. YPI, FL and PAW: supervision. AHD: writing—original draft. AHD, RMM, YPI, FL and PAW: writing—review and editing.

Compliance with ethical standards

Conflict of interest The authors have no conflicts of interest to disclose.

References

Alexander RM (1995) Tendon elasticity and positional control. Behav Brain Sci 18:745. https://doi.org/10.1017/S0140525X00040711

Asmussen E, Bonde-Petersen F (1974) Apparent efficiency and storage of elastic energy in human muscles during exercise. Acta Physiol Scand 92:537–545. https://doi.org/10.1111/j.1748-1716.1974.tb05776.x

Avogadro P, Kyröläinen H, Belli A (2004) Influence of mechanical and metabolic strain on the oxygen consumption slow component during forward pulled running. Eur J Appl Physiol 93:203–209. https://doi.org/10.1007/s00421-004-1200-8

Bhat SG, Cherangara S, Olson J, Redkar S, Sugar TG (2019) Analysis of a periodic force applied to the trunk to assist walking gait. In: WearRAcon, pp 68–73. https://doi.org/10.1109/wearracon.2019.8719396

Burnett DR, Campbell-Kyureghyan NH, Cerrito PB, Quesada PM (2011) Symmetry of ground reaction forces and muscle activity in asymptomatic subjects during walking, sit-to-stand, and stand-to-sit tasks. J Electromyogr Kinesiol 21:610–615. https://doi.org/10.1016/j.jelekin.2011.03.006

Cappellini G, Ivanenko YP, Dominici N et al (2010) Migration of motor pool activity in the spinal cord reflects body mechanics in human locomotion. J Neurophysiol 104:3064–3073. https://doi.org/10.1152/jn.00318.2010

Cappellini G, Ivanenko YP, Martino G et al (2016) Immature spinal locomotor output in children with cerebral palsy. Front Physiol. https://doi.org/10.3389/fphys.2016.00478

Cavagna GA (1975) Force platforms as ergometers. J Appl Physiol 39:174–179

Cavagna GA, Thys H, Zamboni A (1976) The sources of external work in level walking and running. J Physiol 262:639–657. https://doi.org/10.1113/jphysiol.1976.sp011613

Cavagna GA, Willems PA, Legramandi MA, Heglund NC (2002) Pendular energy transduction within the step in human walking. J Exp Biol 205:3413–3422

Chang Y-H, Kram R (1999) Metabolic cost of generating horizontal forces during human running. J Appl Physiol 86:1657–1662. https://doi.org/10.1152/jappl.1999.86.5.1657

Chvatal SA, Torres-Oviedo G, Safavynia SA, Ting LH (2011) Common muscle synergies for control of center of mass and force in nonstepping and stepping postural behaviors. J Neurophysiol 106:999–1015. https://doi.org/10.1152/jn.00549.2010

Conway KA, Bissette RG, Franz JR (2018) The functional utilization of propulsive capacity during human walking. J Appl Biomech 34:474–482. https://doi.org/10.1123/jab.2017-0389

Dewolf AH, Willems PA (2019) Running on a slope: a collision-based analysis to assess the optimal slope. J Biomech 83:298–304. https://doi.org/10.1016/j.jbiomech.2018.12.024

Dewolf AH, Peñailillo LE, Willems PA (2016) The rebound of the body during uphill and downhill running at different speeds. J Exp Biol 219:2276–2288. https://doi.org/10.1242/jeb.142976

Dewolf AH, Ivanenko YP, Lacquaniti F, Willems PA (2017) Pendular energy transduction within the step during human walking on slopes at different speeds. PLoS One. https://doi.org/10.1371/journal.pone.0186963

Dewolf AH, Ivanenko YP, Zelik KE, Lacquaniti F, Willems PA (2018) Kinematic patterns while walking on a slope at different speeds. J Appl Physiol 125:642–653. https://doi.org/10.1152/japplphysiol.01020.2017

Dewolf AH, Ivanenko Y, Zelik KE et al (2019) Differential activation of lumbar and sacral motor pools during walking at different speeds and slopes. J Neurophysiol. https://doi.org/10.1152/jn.00167.2019

Dionisio VC, Hurt CP, Brown DA (2018) Effect of forward-directed aiding force on gait mechanics in healthy young adults while walking faster. Gait Posture 64:12–17. https://doi.org/10.1016/j.gaitpost.2018.05.018

Ellis RG, Sumner BJ, Kram R (2014) Muscle contributions to propulsion and braking during walking and running: insight from external force perturbations. Gait Posture 40:594–599. https://doi.org/10.1016/j.gaitpost.2014.07.002

Franz JR, Kram R (2013) Advanced age affects the individual leg mechanics of level, uphill, and downhill walking. J Biomech 46:535–540. https://doi.org/10.1016/j.jbiomech.2012.09.032

Fuchioka S, Iwata A, Higuchi Y et al (2015) The forward velocity of the center of pressure in the midfoot is a major predictor of gait speed in older adults. Int J Gerontol 9:119–122. https://doi.org/10.1016/j.ijge.2015.05.010

Gill ML, Grahn PJ, Calvert JS et al (2018) Neuromodulation of lumbosacral spinal networks enables independent stepping after complete paraplegia. Nat Med 24:1677–1682. https://doi.org/10.1038/s41591-018-0175-7

Gimenez P, Arnal PJ, Samozino P et al (2014) Simulation of uphill/downhill running on a level treadmill using additional horizontal force. J Biomech 47:2517–2521. https://doi.org/10.1016/j.jbiomech.2014.04.012

Gottschall JS, Kram R (2003) Energy cost and muscular activity required for propulsion during walking. J Appl Physiol 94:1766–1772. https://doi.org/10.1152/japplphysiol.00670.2002

Gottschall JS, Kram R (2006) Mechanical energy fluctuations during hill walking: the effects of slope on inverted pendulum exchange. J Exp Biol 209:4895–4900. https://doi.org/10.1242/jeb.02584

Grabowski AM, Kram R (2008) Running with horizontal pulling forces: the benefits of towing. Eur J Appl Physiol 104:473–479. https://doi.org/10.1007/s00421-008-0785-8

Hsiao H, Knarr BA, Higginson JS, Binder-Macleod SA (2015) Mechanisms to increase propulsive force for individuals poststroke. J Neuroeng Rehabilit. https://doi.org/10.1186/s12984-015-0030-8

Ivanenko YP, Poppele RE, Lacquaniti F (2006) Spinal cord maps of spatiotemporal alpha-motoneuron activation in humans walking at different speeds. J Neurophysiol 95:602–618. https://doi.org/10.1152/jn.00767.2005

Ivanenko YP, Cappellini G, Poppele RE, Lacquaniti F (2008) Spatiotemporal organization of α-motoneuron activity in the human spinal cord during different gaits and gait transitions. Eur J Neurosci 27:3351–3368. https://doi.org/10.1111/j.1460-9568.2008.06289.x

Ivanenko YP, Dominici N, Cappellini G et al (2013) Changes in the spinal segmental motor output for stepping during development from infant to adult. J Neurosci 33:3025–3036a

Kendall F, McCreary E, Provance P et al (2005) Muscles. Testing and function with posture and pain. Lippincott Williams and Wilkins, Baltimore

Kurz MJ, Stergiou N (2007) Do horizontal propulsive forces influence the nonlinear structure of locomotion? J Neuroeng Rehabilit. https://doi.org/10.1186/1743-0003-4-30

La Scaleia V, Ivanenko YP, Zelik KE, Lacquaniti F (2014) Spinal motor outputs during step-to-step transitions of diverse human gaits. Front Hum Neurosci 8:305. https://doi.org/10.3389/fnhum.2014.00305

Lejeune TM, Willems PA, Heglund NC (1998) Mechanics and energetics of human locomotion on sand. J Exp Biol 201(13):2071–2080

Lenzo B, Zanotto D, Vashista V et al (2014) A new constant pushing force device for human walking analysis. In: IEEE international conference on robotics and automation, pp 6174–6179. https://doi.org/10.1109/ICRA.2014.6907769

Maclellan MJ, Ivanenko YP, Massaad F et al (2014) Muscle activation patterns are bilaterally linked during split-belt treadmill walking in humans. J Neurophysiol 111:1541–1552. https://doi.org/10.1152/jn.00437.2013

Margaria R (1968) Positive and negative work performances and their efficiencies in human locomotion. Int Z Angew Physiol Einschl Arbeitsphysiol 25:339–351. https://doi.org/10.1007/BF00699624

Martino G, Ivanenko Y, Serrao M, Ranavolo A, Draicchio F, Rinaldi M, Casali C, Lacquaniti F (2018) Differential changes in the spinal segmental locomotor output in hereditary spastic paraplegia. Clin Neurophysiol 129:516–525. https://doi.org/10.1016/j.clinph.2017.11.028

Meurisse GM, Dierick F, Schepens B, Bastien GJ (2016) Determination of the vertical ground reaction forces acting upon individual limbs during healthy and clinical gait. Gait Posture 43:245–250. https://doi.org/10.1016/j.gaitpost.2015.10.005

Mignardot J-B, Le Goff CG, Van Den Brand R et al (2017) A multidirectional gravity-assist algorithm that enhances locomotor control in patients with stroke or spinal cord injury. Sci Transl Med. https://doi.org/10.1126/scitranslmed.aah3621

Minetti AE, Ardigò LP, Saibene F (1993) Mechanical determinants of gradient walking energetics in man. J Physiol 472:725–735. https://doi.org/10.1113/jphysiol.1993.sp019969

Na K-P, Kim YL, Lee SM (2015) Effects of gait training with horizontal impeding force on gait and balance of stroke patients. J Phys Ther Sci 27:733–736. https://doi.org/10.1589/jpts.27.733

Naidu A, Graham SA, Brown D (2019) Fore-aft resistance applied at the center of mass using a novel robotic interface proportionately increases propulsive force generation in healthy nonimpaired individuals walking at a constant speed. J Neuroeng Rehabil 16:111

Penke K, Scott K, Sinskey Y, Lewek MD (2019) Propulsive forces applied to the body's center of mass affect metabolic energetics poststroke. Arch Phys Med Rehabil 100:1068–1075. https://doi.org/10.1016/j.apmr.2018.10.010

Pierotti SE, Brand RA, Gabel RH et al (1991) Are leg electromyogram profiles symmetrical? J Orthop Res 9:720–729. https://doi.org/10.1002/jor.1100090512

Prampero PED, Fusi S, Sepulcri L et al (2005) Sprint running: a new energetic approach. J Exp Biol 208:2809–2816. https://doi.org/10.1242/jeb.01700

Pugh LGCE (1971) The influence of wind resistance in running and walking and the mechanical efficiency of work against horizontal or vertical forces. J Physiol 213:255–276. https://doi.org/10.1113/jphysiol.1971.sp009381

Sadeghi H, Allard P, Prince F, Labelle H (2000) Symmetry and limb dominance in able-bodied gait: a review. Gait Posture 12:34–45

Saunders JB, Inman VT, Eberhart HB (1953) The major determinants in normal and pathological gait. J Bone Jt Surg Am 35A:543–558. https://doi.org/10.2106/00004623-195335030-00003

Sayenko DG, Rath M, Ferguson AR et al (2019) Self-assisted standing enabled by non-invasive spinal stimulation after spinal cord injury. J Neurotrauma 36:1435–1450. https://doi.org/10.1089/neu.2018.5956

Simha SN, Wong JD, Selinger JC, Donelan JM (2019) A mechatronic system for studying energy optimization during walking. IEEE Trans Neural Syst Rehabil Eng 27(7):1416–1425. https://doi.org/10.1109/TNSRE.2019.2917424

Solopova IA, Sukhotina IA, Zhvansky DS et al (2017) Effects of spinal cord stimulation on motor functions in children with cerebral palsy. Neurosci Lett 639:192–198. https://doi.org/10.1016/j.neulet.2017.01.003

Sun J, Walters M, Svensson N, Lloyd D (1996) The influence of surface slope on human gait characteristics: a study of urban pedestrians walking on an inclined surface. Ergonomics 39:677–692. https://doi.org/10.1080/00140139608964489

Tomlinson BE, Irving D (1977) The numbers of limb motor neurons in the human lumbosacral cord throughout life. J Neurol Sci 34:213–219

Usherwood JR, Szymanek KL, Daley MA (2008) Compass gait mechanics account for top walking speeds in ducks and humans. J Exp Biol 211:3744–3749. https://doi.org/10.1242/jeb.023416

Van Caekenberghe I, Segers V, Willems P et al (2013) Mechanics of overground accelerated running vs. running on an accelerated treadmill. Gait Posture 38:125–131. https://doi.org/10.1016/j.gaitpost.2012.10.022

Wagner FB, Mignardot J-B, Le Goff-Mignardot CG et al (2018) Targeted neurotechnology restores walking in humans with spinal cord injury. Nature 563:65–71. https://doi.org/10.1038/s41586-018-0649-2

Wang J, Hurt CP, Capo-Lugo CE, Brown DA (2015) Characteristics of horizontal force generation for individuals post-stroke walking against progressive resistive forces. Clin Biomech 30:40–45. https://doi.org/10.1016/j.clinbiomech.2014.11.006

Winter DA (1991) The biomechanics and motor control of human gait: normal, elderly and pathological. Waterloo Biomechanics, Waterloo

Zirker CA, Bennett BC, Abel MF (2013) Changes in kinematics, metabolic cost and external work during walking with a forward assistive force. J Appl Biomech 29:481–489. https://doi.org/10.1123/jab.29.4.481